Table 1
$V_{0.5}$, slope factor k and τ deactivation at +20 mV.

	N	$V_{0.5}$	k	τ_{fast}	τ_{slow}
***KCNH2*-WT**	32	−18.515 ± 0.961	9.370 ± 0.437	0.184 ± 0.008	1.098 ± 0.047
***KCNH2*-WT/E58K**	34	−18.590 ± 1.200	7.993 ± 0.309*	0.174 ± 0.010	1.050 ± 0.064
***KCNH2*-E58K**	12	−35.847 ± 2.060*	6.766 ± 0.506**	0.118 ± 0.024*	0.834 ± 0.141*
***KCNH2*-WT+*KCNE1*-WT**	23	−18.326 ± 0.775	7.373 ± 0.289	0.183 ± 0.016	1.077 ± 0.102
***KCNH2*-WT+*KCNE1*-D85N**	20	−22.069 ± 1.560***	7.037 ± 0.389	0.193 ± 0.013	1.258 ± 0.090
***KCNH2*-WT/E58K+*KCNE1*-D85N**	15	−24.467 ± 2.122***	7.525 ± 0.947	0.212 ± 0.033	1.092 ± 0.149

* $P < 0.05$ vs. *KCNH2*-WT.
** $P < 0.05$ vs. *KCNH2*-WT+*KCNE1*-WT.
*** $P < 0.005$ vs. *KCNH2*-WT+*KCNE1*-WT.

rectifying outward currents in response to depolarization pulses and slowly deactivating tail currents (Fig. 2A). Cells transfected with *KCNH2*-E58K alone produced very small outward currents (Fig. 2C). Compared to *KCNH2*-WT, *KCNH2*-WT/E58K had reduced peak tail currents by 25–28% at test potentials between 0 and +50 mV, although there was no statistical significance. Moreover, fitting of normalized data to Boltzmann's equation yielded a $V_{0.5}$ of −18.5 ± 1.0 mV for *KCNH2*-WT and of −18.6 ± 1.2 mV for *KCNH2*-WT/E58K that were not significantly different. Deactivation of tail currents could be fitted by 2 exponentials, yielding fast and slow time constants (τ_{fast} and τ_{slow}). The deactivation time constants were not significantly different between the 2 current–voltage relationships (Table 1). Taken together, the KCNH2 mutation showed no apparent dominant negative suppression effects.

We then examined how *KCNE1* and its D85N variant influence the I_{Kr} currents. Fig. 3A-a and b depict 2 sets of current traces recorded from CHO cells transfected with *KCNH2*-WT plus *KCNE1*-WT or *KCNE1*-D85N (1 μg each). Lower panel c shows current traces recorded from a cell transfected with *KCNH2*-WT and *KCNH2*-E58K (0.5 μg each, total 1 μg) and *KCNE1*-D85N (1 μg), which mimics the pathological condition of the index patients.

Peak tail current densities measured at −60 mV were calculated in the respective cells and are plotted as a function of test potential in Fig. 3B. Compared to *KCNE1*-WT, *KCNE1*-D85N reduced the peak tail currents by 31–36% at test potentials between 0 and +50 mV ($P < 0.005$ vs. *KCNH2*-WT plus *KCNE1*-WT). *KCNH2*-WT/E58K plus *KCNE1*-D85N reduced peak tail currents by 60–65% at test potentials between 0 and +50 mV ($P < 0.0001$ vs. *KCNH2*-WT plus *KCNE1*-WT). Fitting of normalized data to Boltzmann's equation yielded a $V_{0.5}$ of −18.3 ± 0.8 mV for *KCNH2*-WT/*KCNE1*-WT, of −22.1 ± 1.6 mV for *KCNH2*-WT/*KCNE1*-D85N ($P < 0.05$), and of −24.5 ± 2.1 mV for *KCNH2*-WT/E58K plus *KCNE1*-D85N ($P < 0.005$). These data suggest that the presence of both *KCNH2*-E58K and *KCNE1*-D85N caused a significantly negative shift of I_{Kr} activation kinetics (Fig. 3C and Table 1). Fast and slow deactivation time constants (τ_{fast} and τ_{slow}) were not significantly different between the 2 types of I_{Kr} (Table 1).

4. Discussion

The present study provides clinical, molecular, and in vitro electrophysiological evidence that a rare SNP (*KCNE1*-D85N) can act as a genetic modifier in LQTS. In general, SNPs are thought to be non-pathological, but some have been reported to modify the clinical features of the disease. For example, the *KCNH2*-K897T polymorphism [8] has been shown to aggravate LQTS phenotypes directly by reducing cardiac K^+ channel function in association with the *KCNH2* mutation, A1116V. The prevalence of the *KCNH2*-K897T polymorphism is estimated to be up to 33% in Caucasians [10,12,13].

A rare genetic variant of LQTS, *KCNE1*-D85N, was originally reported by Tesson et al. [14], and we have previously demonstrated that the prevalence of the SNP is 0.8% in healthy Japanese individuals and 3.9% in clinically diagnosed LQTS probands [9]. In a heterologous expression system with *Xenopus* oocytes, *KCNE1*-D85N has been shown to reduce I_{Ks} by approximately 50% [5]. In our previous experiments [9] using CHO cells, D85N also significantly reduced I_{Ks} by 28% ($P < 0.05$ vs. WT), although this was a smaller reduction than that shown in *Xenopus* oocytes [5]. In contrast, when *KCNH2*-WT was co-expressed with the variant, it was found to decrease I_{Kr} significantly by 31–36% ($P < 0.005$ vs. WT) [9]. Regarding the current reduction, the interaction between KCNE1 and KCNH2 was, therefore, stronger than that between KCNE1 and KCNQ1. Since in the range of a normal heart rate I_{Kr} plays a more essential role for ventricular repolarization than I_{Ks}, carriers of loss-of-function *KCNH2* mutations generally display longer QT prolongation and bradycardia than those of *KCNQ1* mutations.

The present study attests that 3.9% of the LQTS subjects genotyped had the *KCNE1*-D85N variant in addition to a LQT-related mutation. The average QT interval of *KCNE1*-D85N carriers was longer than that of non-carriers. The incidence of symptoms in patients with *KCNE1*-D85N was higher than that of the patients without *KCNE1*-D85N, although the differences were not significant. Here, we clinically evaluated the family members as a group with a relatively homogeneous genetic background and/or the same mutation, *KCNH2*-E58K, to show that the *KCNE1*-D85N polymorphism could act as a modifier. In fact, the proband and her daughter carried both *KCNH2*-E58K and *KCNE1*-D85N and had a longer QT interval than the proband's son, who carried *KCNH2*-E58K only. In a biophysical assay, *KCNH2*-WT/E58K induced a small decrease in current densities, compared to *KCNH2*-WT, suggesting no dominant negative suppression, but a small mutant effect (Fig. 2). Co-expression of *KCNH2*-WT with/without *KCNH2*-E58K and *KCNE1*-D85N showed a significantly negative shift of the activation curve compared to *KCNH2*-WT with *KCNE1*-WT (−6 mV and −4 mV, respectively); in other words, a gain of function. However, there was a massive decrease in current densities by *KCNE1*-D85N, about 60–65% ($P < 0.0001$ vs. *KCNH2*-E58K and *KCNE1*-WT; Fig. 3B). Therefore, the latter change led to a loss-of-function effect by *KCNE1*-D85N. The proband and her daughter carried both these 2 genetic variants and both of them experienced TdP resulting in repeated syncope. From these clinical features, the D85N variant was suggested to aggravate the clinical phenotypes by largely reducing I_{Kr}. Thus, loss-of-function effects caused by the combination of the 2 genetic variants may explain the significant prolongation of the QTc intervals and the severe symptoms in the family.

More recently, Yoshikane and his colleagues [15] reported a family in which 2 genetic variants were harbored in the presence or absence of the *KCNE1*-D85N polymorphism. They compared the symptoms among the family members who carried one or more of the genetic variants *KCNH2*-N45D, *SCN5A*-A1428S, or *KCNE*1-D85N. They demonstrated that only the proband carrying all 3 variants (triple hit) experienced ventricular fibrillation, and his ECG showed marked bradycardia. His brother and mother carried either *KCNH2*-N45D or *SCN5A*-A1428S, in addition to *KCNE1*-D85N (double hit). His father carried only *KCNH2*-N45D. All family members except for the proband

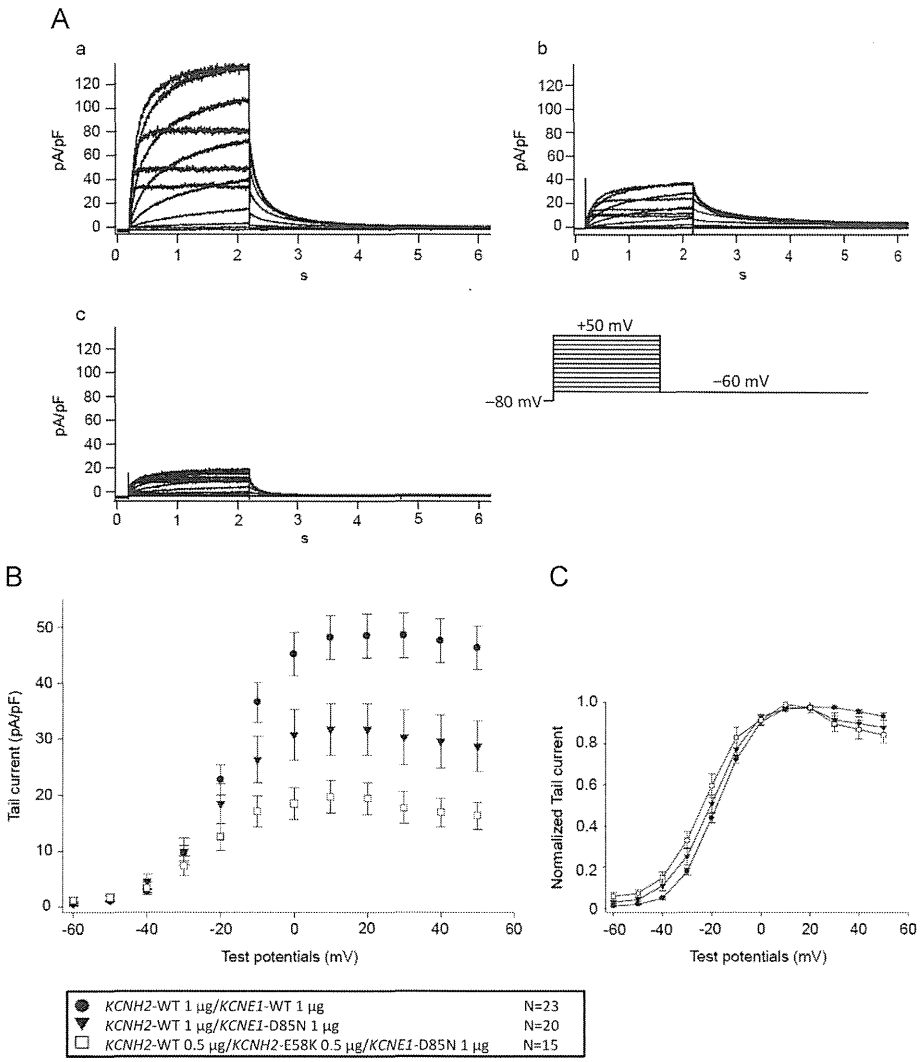

Fig. 3. Functional expression analysis of *KCNH2* with *KCNE1* in Chinese hamster ovary cells. A: Representative current traces of *KCNH2* WT and/or E58K co-expression with *KCNE1*-WT or *KCNE1*-D85N. (a) *KCNH2*-WT (1 μg) plus *KCNE1*-WT (1 μg). (b) *KCNH2*-WT (1 μg) plus *KCNE1*-D85N (1 μg) ($P < 0.005$ vs. *KCNH2*-WT (1 μg) plus *KCNE1*-WT (1 μg)). (c) *KCNH2*-WT/E58K (0.5 μg of each, total 1 μg) plus *KCNE1*-D85N (1 μg) ($P < 0.0001$ vs. *KCNH2*-WT (1 μg) plus *KCNE1*-WT (1 μg)). (B and C) Functional consequences of *KCNH2* WT and/or E58K with *KCNE1*-WT or D85N ([B] activation curve; [C] normalized activation curve). Solid circles indicate data from 23 cells that were transfected with *KCNH2*-WT (1 μg) plus *KCNE1*-WT (1 μg). Solid triangles indicate data from 20 cells that were transfected with *KCNH2*-WT (1 μg) plus *KCNE1*-D85N (1 μg). Open squares indicate data from 15 cells that were transfected with *KCNH2*-WT/E58K (0.5 μg each, total 1 μg) and *KCNE1*-D85N (1 μg).

remained asymptomatic. When compared, the phenotype of the proband's brother and father (both carry *KCNH2*-N45D, but D85N is present only in the brother), the QTc intervals were longer in the brother (500 vs. 430 ms) and a Holter ECG revealed the presence of bradycardia in the brother. Thus, *KCNE1*-D85N appeared to modify the disease phenotypes, providing another example of D85N as a genetic modifier of LQTS.

In conclusion, a rare *KCNE1*-D85N polymorphism may modify the LQTS phenotype in combination with other pathogenic LQTS-related gene mutations.

Disclosures

This work was supported by Grants-in-Aid in Scientific Research from the Ministry of Education, Culture, Science, and Technology of Japan, a Health Sciences Research Grant from the Ministry of Health, Labor, and Welfare of Japan, and Translational Research Funds from the Japan Circulation Society.

Conflict of interest

There are no conflicts of interest.

Acknowledgments

The authors are grateful to the Japanese LQT families for their willingness to participate in this study and to Dr. Y. Yoshikane and Dr. M. Yoshinaga for keen discussion. We thank Arisa Ikeda, Kazu Toyooka, and Aya Umehara for excellent technical assistance.

References

[1] Keating MT, Sanguinetti MC. Molecular and cellular mechanisms of cardiac arrhythmias. Cell 2001;104:569–80.
[2] Shimizu W. Clinical impact of genetic studies in lethal inherited cardiac arrhythmias. Circ J 2008;72:1926–36.
[3] Goldenberg I, Moss AJ. Long QT syndrome. J Am Coll Cardiol 2008;51: 2291–2300.
[4] Chen L, Marquardt ML, Tester DJ, et al. Mutation of an A-kinase-anchoring protein causes long-QT syndrome. Proc Natl Acad Sci USA 2007;104:20990–5.
[5] Westenskow P, Splawski I, Timothy KW, et al. Compound mutations: a common cause of severe long-QT syndrome. Circulation 2004;109:1834–41.
[6] Schwartz PJ, Priori SG, Napolitano C. How really rare are rare diseases?: The intriguing case of independent compound mutations in the long QT syndrome J Cardiovasc Electrophysiol 2003;14:1120–1.
[7] Itoh H, Shimizu W, Hayashi K, et al. Long QT syndrome with compound mutations is associated with a more severe phenotype: a Japanese multicenter study. Heart Rhythm 2010;7:1411–8.
[8] Crotti L, Lundquist AL, Insolia R, et al. KCNH2-K897T is a genetic modifier of latent congenital long-QT syndrome. Circulation 2005;112:1251–8.
[9] Nishio Y, Makiyama T, Itoh H, et al. D85N, a KCNE1 polymorphism, is a disease-causing gene variant in long QT syndrome. J Am Coll Cardiol 2009;54: 812–819.
[10] Ackerman MJ, Tester DJ, Jones GS, et al. Ethnic differences in cardiac potassium channel variants: implications for genetic susceptibility to sudden cardiac death and genetic testing for congenital long QT syndrome. Mayo Clin Proc 2003;78:1479–87.
[11] Paulussen AD, Gilissen RA, Armstrong M, et al. Genetic variations of KCNQ1, KCNH2, SCN5A, KCNE1, and KCNE2 in drug-induced long QT syndrome patients. J Mol Med (Berl) 2004;82:182–8.
[12] Bezzina CR, Verkerk AO, Busjahn A, et al. A common polymorphism in KCNH2 (HERG) hastens cardiac repolarization. Cardiovasc Res 2003;59:27–36.
[13] Paavonen KJ, Chapman H, Laitinen PJ, et al. Functional characterization of the common amino acid 897 polymorphism of the cardiac potassium channel KCNH2 (HERG). Cardiovasc Res 2003;59:603–11.
[14] Tesson F, Donger C, Denjoy I, et al. Exclusion of KCNE1 (IsK) as a candidate gene for Jervell and Lange-Nielsen syndrome. J Mol Cell Cardiol 1996;28: 2051–2055.
[15] Yoshikane Y, Yoshinaga M, Hamamoto K, et al. A case of long QT syndrome with triple gene abnormalities: Digenic mutations in KCNH2 and SCN5A and gene variant in KCNE1. Heart Rhythm 2013;10:600–3.

ORIGINAL ARTICLE

Additional diagnostic value of first-pass myocardial perfusion imaging without stress when combined with 64-row detector coronary CT angiography in patients with coronary artery disease

Kazuhiro Osawa,[1] Toru Miyoshi,[2] Yasushi Koyama,[3] Katsushi Hashimoto,[1] Shuhei Sato,[4] Kazufumi Nakamura,[1] Nobuhiro Nishii,[1] Kunihisa Kohno,[1] Hiroshi Morita,[2] Susumu Kanazawa,[4] Hiroshi Ito[1]

► Additional material is published online only. To view please visit the journal online (http://dx.doi.org/10.1136/heartjnl-2013-305468).

[1]Department of Cardiovascular Medicine, Okayama University Graduate School of Medicine, Dentistry and Pharmaceutical Sciences, Okayama, Japan
[2]Department of Cardiovascular Therapeutics, Okayama University Graduate School of Medicine, Dentistry and Pharmaceutical Sciences, Okayama, Japan
[3]Cardiovascular Center, Sakurabashi-Watanabe Hospital, Umeda, Osaka, Japan
[4]Department of Radiology, Okayama University Graduate School of Medicine, Dentistry and Pharmaceutical Sciences, Okayama, Japan

Correspondence to
Toru Miyoshi, Department of Cardiovascular Therapeutics, Okayama University Graduate School of Medicine, Dentistry and Pharmaceutical Sciences, 2-5-1 Shikata-cho, Okayama 700-8558, Japan; miyoshit@cc.okayama-u.ac.jp

Received 2 January 2014
Revised 24 March 2014
Accepted 29 March 2014
Published Online First 24 April 2014

To cite: Osawa K, Miyoshi T, Koyama Y, *et al*. *Heart* 2014;**100**: 1008–1015.

ABSTRACT

Objective Multi-detector coronary CT angiography (CCTA) can detect coronary stenosis, but it has a limited ability to evaluate myocardial perfusion. We evaluated the usefulness of first-pass CT-myocardial perfusion imaging (MPI) in combination with CCTA for diagnosing coronary artery disease (CAD).

Methods A total of 145 patients with suspected CAD were enrolled. We used 64-row multi-detector CT (Definition Flash, Siemens). The same coronary CCTA data were used for first-pass CT-MPI without drug loading. Images were reconstructed by examining the signal densities at diastole as colour maps. Diagnostic accuracy was assessed by comparison with invasive coronary angiography.

Results First-pass CT-MPI in combination with CCTA significantly improved diagnostic performance compared with CCTA alone. With per-vessel analysis, the sensitivity, specificity, positive predictive value and negative predictive value increased from 81% to 85%, 87% to 94%, 63% to 79% and 95% to 96%, respectively. The area under the receiver operating characteristic curve for detecting CAD also increased from 0.84 to 0.89 (p=0.02). First-pass CT-MPI was particularly useful for assessing segments that could not be directly evaluated due to severe calcification and motion artefacts.

Conclusions First-pass CT-MPI has an additional diagnostic value for detecting coronary stenosis, in particular in patients with severe calcification.

INTRODUCTION

Coronary CT angiography (CCTA) using 64-row detector CT is a feasible non-invasive modality for detecting coronary artery disease (CAD).[1] Despite this excellent performance, CCTA has limitations in cases of severe calcified coronary arteries and has substantial motion artefacts. To overcome these problems, stress single-photon emission CT (SPECT),[2] stress echocardiography[3] and MRI[4] have been used simultaneously. Recent studies demonstrated that pharmacological adenosine stress CT myocardial perfusion imaging (MPI) is a promising method for the detection of CAD;[5] however, this method requires additional contrast medium and radiation exposure.

A previous study showed that myocardial perfusion without stress is affected by coronary stenosis.[6] Coronary capillary microvessels autoregulate their hydrostatic blood pressure to maintain homeostasis. With moderate levels of coronary stenosis, the epicardial coronary pressure remains constant by increasing capillary resistance in the corresponding myocardial territory.[7] In individuals without myocardial infarction, when coronary stenosis becomes severe, the decrease in myocardial blood volume becomes prominent because a large amount of the perfusion bed shuts down, which is seen as attenuation of myocardial perfusion on first-pass CT-MPI.

We applied this theory to CCTA. We reconstructed first-pass CT-MPI data that were simultaneously acquired during CCTA in patients with suspected CAD. The purpose of this study was to evaluate the feasibility and diagnostic accuracy of first-pass CT-MPI without stress for detecting clinically important coronary artery stenosis compared with invasive coronary angiography, which was the reference standard.

METHODS

Detailed methods are provided in the online supplementary appendix.

Study design and patient population

This study population consisted of consecutive patients with suspected CAD who underwent CCTA at Okayama University Hospital between August 2011 and December 2012 (figure 1). The following candidates were excluded: Patients with acute clinical instability, contraindications to iodinated contrast material (known allergy or serum creatine level >1.5 mg/dL), non-sinus rhythm, previous myocardial infarction, evidence of Q waves on resting electrocardiography, previous coronary stent implantation and previous coronary artery bypass graft surgery. In total, 145 patients were enrolled in this study. All patients underwent CCTA and invasive coronary angiography within 30 days. First-pass CT-MPI was simultaneously obtained during CCTA in all patients. Among the 145 patients, 35 also underwent a nuclear stress test within 30 days. This study was approved by the

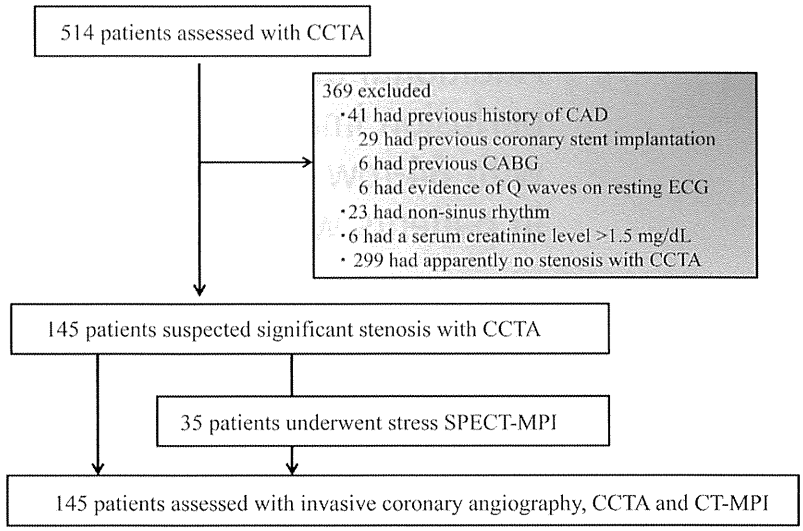

Figure 1 Flow diagram of patient recruitment.

institutional ethics committee on human research. Written informed consent was given by all patients before the study. This study was conducted in accordance with the latest version of the Declaration of Helsinki.

Imaging acquisition

CT protocol

We obtained 128-slice CT scans using a DCT scanner (SOMATOM Definition Flash, Siemens Medical Solutions, Germany).[8]

First-pass CT-MPI

Retrospective image reconstruction was performed at 5% phase increments throughout the cardiac cycle. A total of 20 image data sets were reconstructed. The slice thickness was 3 mm. The short-axis images were reconstructed from 20 image data sets using the standard double oblique method. The images were analysed with a commercially available cardiac evaluation software program (Cardiac CT Image Report CIR-SV03, bundled software Vascular Volume Mapping, Siemens compatible V.1.0, ARGUS B.M.C., Ehime, Japan).

Nuclear stress testing

All stress and rest nuclear SPECT examinations were performed according to standard institutional clinical protocols with ^{99m}Tc or ^{201}Tl as the tracer using a dual detector cardiac gamma camera (DISCOVERY, NM/CT 670 GE Healthcare).

Invasive coronary artery angiography

Invasive coronary artery angiography was performed by one experienced senior cardiologist (HK) according to standard procedures using the transradial Judkin's technique. To visualise the left coronary artery, at least six projections were obtained; for the right coronary artery (RCA), at least four projections were obtained.

Image processing and interpretation

Reference standard: quantitative coronary angiography

Quantitative coronary artery angiography analysis was performed to determine the per cent stenosis in each coronary segment. Coronary artery stenosis was defined as 'significant' if the mean luminal diameter narrowing exceeded 50%.

Coronary artery CT angiography: CCTA

The presence of coronary artery stenosis was defined as a luminal obstruction of greater than 50% of the diameter. All coronary artery segments were assessed for the presence of significant stenosis.

CT-MPI

The same raw data used for CCTA were used to create short-axis images via reconstruction at the mid-diastolic to end-diastolic phase of the cardiac cycle and were finally expressed in a bulls-eye map. Assignment of the left ventricular segment was based on the 16 myocardial segment models, excluding the apical segment.[9] Perfusion imaging was expressed with colour maps coded according to the CT value.

SPECT-MPI

Data were evaluated using short-axial, horizontal long-axial and vertical long-axial source images. Gated SPECT data, if acquired, were also presented to the readers. Disagreements in data analysis between the two observers were resolved by consensus reading.

Matching of perfusion-based segments to the corresponding vascular territory

To ensure correct association of the myocardial segments with the correct vascular territory, angiographic visualisation of vessel dominance was used to decide which vessel supplied the inferior and inferoseptal territories. Moreover, we also considered which vessel, diagonal branch or obtuse marginal branch was dominant in the basal to mid-anterolateral wall.

Radiation dose estimates of CT

We calculated the effective radiation dose for each component of the cardiac CT examination by multiplying the dose-length product by a conversion coefficient for the chest (k=0.014 mSV/mGy/cm).[8]

Statistical analysis

All continuous variables are presented as the mean±SD, and categorical variables are expressed as frequencies or percentages. The inter-observer coefficient of variation was <5% as assessed in 20 randomly selected samples. With invasive coronary angiography as the primary reference, the diagnostic accuracies of CCTA, CT-MPI, CCTA plus CT-MPI, and SPECT-MPI were expressed in terms of sensitivity, specificity, positive predictive value (PPV) and negative predictive value (NPV) for the detection of vascular territories with significant obstructive coronary artery stenosis. Diagnostic performance was calculated on a per-vessel and per-patient basis. The vessel-based analysis included the RCA, left anterior descending (LAD) artery and left circumflex artery (LCX) in all patients. CCTA diagnosis was reclassified according to CT-MPI analysis (figure 2). The area under the receiver operating characteristic (ROC) curve (C statistic) was calculated for all diagnostic testing strategies for which a reference standard was available. A p value <0.05 was considered statistically significant. The area under the ROC curve was compared using the ROCCOMP command (Stata V.10; StataCorp, College Station, Texas, USA). Other statistical analyses were performed using SPSS V.17.0 for Windows (SPSS Inc., Chicago, Illinois, USA).

RESULTS

Study population

Clinical characteristics of the study population are shown in table 1. Of the 145 study participants (mean age 65.7 ±12.4 years, 61% men), 31% had diabetes mellitus and 24% were current smokers. The average volume of the contrast dose for CT-MPI and CCTA was 70±12 mL. The average effective radiation dose for cardiac CT examination was 14.8±2.9 mSV. The average radiation dose for stress SPECT was 4.5±0.6 mGy with ^{99m}Tc (n=31) and 26.3±5.8 mGy with ^{201}Tl (n=4).

Invasive coronary angiography

Invasive coronary artery angiography showed that 49 (34%) patients had more than 50% stenosis in at least one coronary artery. Of the 49 patients with stenotic vessels as determined with invasive coronary angiography, 19 (39%) had single-vessel disease, 18 (37%) had double-vessel disease and 12 (24%) had triple-vessel disease. On a per-vessel basis, 91 of the 435 vessels had significant stenosis. Among the 91 stenotic vessels, 38 (42%) were in the LAD, 25 (27%) were in the LCX and 28 (31%) were in the RCA.

Analysis in all patients

Representative images of CCTA, CT-MPI, stress SPECT-MPI, invasive of coronary angiography, and short-axial and long-axial left ventricular CT image are presented in figures 3 and 4.

With CCTA, luminal diameter narrowing of more than 50% was diagnosed in 69 (48%) patients and 118 (27%) vessels. Among them, 22 patients had at least one non-evaluable vessel, mainly due to severe calcification. First-pass CT-MPI showed that 48 patients (33%) had perfusion abnormalities, and among 435 vascular territories, 100 (23%) had perfusion abnormalities. Among 21 (5%) vessels with moderate stenosis as seen with CCTA, CT-MPI revealed seven territory defects. Finally, CCTA plus first-pass CT-MPI identified 97 (22%) stenotic vessel territories in 435 vessel territories in 145 patients. Table 2 shows the diagnostic accuracy of CCTA, CT-MPI, and CCTA plus CT-MPI in all patients. CCTA plus first-pass CT-MPI yielded the following results for detecting vascular territories with more than 50% coronary stenosis (as determined with invasive angiography): sensitivity 0.85; specificity 0.94; PPV 0.79; and NPV 0.96. Per-patient results were as follows: sensitivity 0.92; specificity 0.89; PPV 0.80; and NPV 0.96. We observed a significant improvement in the area under the ROC curve for CCTA plus first-pass CT-MPI for distinguishing stenotic coronary arteries compared with CCTA alone, with an increase from 0.84 to 0.89 with per-vessel analysis (p=0.02) and from 0.85 to 0.90 (p=0.04) with per-patient analysis.

Analysis with three modalities—conventional coronary angiography, CCTA plus CT-MPI, and stress SPECT-MPI—in 35 patients

A total of 35 patients were assessed with all three modalities: invasive coronary angiography, CCTA plus CT-MPI, and stress

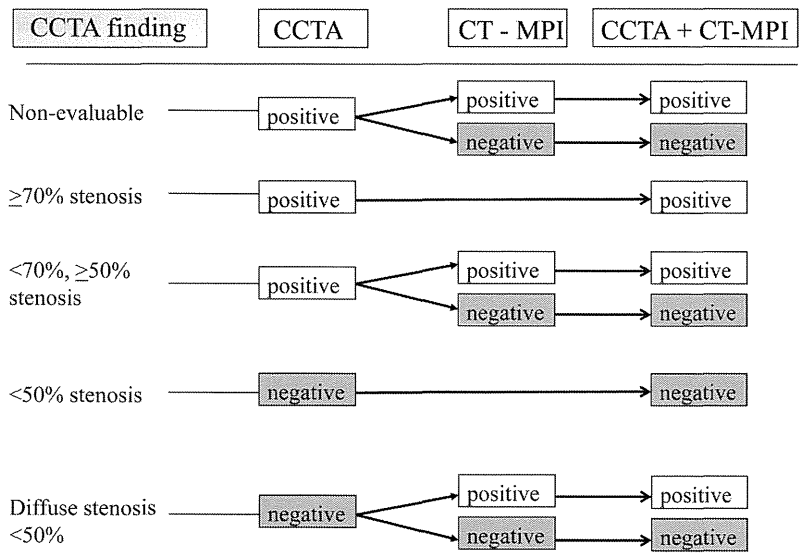

Figure 2 Reclassification criteria. Before CT-myocardial perfusion imaging (CT-MPI) analysis, we defined any vessel that was non-evaluable with coronary CT angiography (CCTA) as positive for stenosis using the following criteria: those with no vessel wall definition owing to marked motion artefacts, significant structural discontinuity, or heavy calcification and high image noise-related blurring that precluded the acquisition of diagnostic information. After the CT-MPI analysis, non-evaluable vessels were considered positive for stenosis only if they corresponded to a CT-MPI defect in the same vascular distribution. Moderate stenoses (50%–70%) on CCTA were reclassified as negative for stenosis if the CT-MPI showed no defect in the same distribution. CCTA stenosis was not reclassified when no stenosis <50% or >70% was apparent on CCTA.

Table 1 Patient characteristics

Age (years)	65.7±12.4
Male sex	88 (61)
Diabetes mellitus	45 (31)
Hypertension	87 (60)
Dyslipidaemia	61 (42)
Body weight (kg)	61±12
Body mass index (kg/m^2)	23.4±3.6
Current smoking	35 (24)
Serum lipid biomarkers (mg/dL)	
Total cholesterol	190.2±35.6
LDL cholesterol	112.6±32.4
HDL cholesterol	55.7±13.6
Serum triglycerides	153.4 (93.5)
Serum creatine (mg/dL)	0.8±0.2
Baseline medications (%)	
β-Blockers	22 (15)
ACEIs/ARBs	58 (40)
Statins	38 (26)
Vital signs	
Systolic blood pressure (mm Hg)	129.6±23.4
Diastolic blood pressure (mm Hg)	75.0±12.4
Heart rate (beats/min)	68.9±12.2

Data are the number (%) or mean±SD.
ACEI, ACE inhibitor; ARB, angiotensin II receptor blocker; HDL, high-density lipoprotein; LDL, low-density lipoprotein.

SPECT-MPI (table 3). In these patients, we investigated the diagnostic accuracy of CCTA plus first-pass CT-MPI compared with stress SPECT-MPI. With invasive coronary artery angiography, 23 (66%) patients had more than 50% stenosis in at least one coronary artery. On a per-vessel basis, 40 of 105 vessels had significant coronary stenosis. Among the 40 stenotic vessels, 18 (45%) were LADs, 11 (28%) were LCXs and 11 (28%) were RCAs. First-pass CT-MPI showed perfusion abnormalities in 50 (48%) vascular territories among 105 vascular territories in 22 (63%) patients. CCTA plus first-pass CT-MPI showed that 54 (51%) among 105 vessels were identified as having significant stenosis in the coronary arteries. The area under the ROC curve for CCTA plus CT-MPI tended to increase from 0.64 to 0.77 with per-patient analysis (p=0.06 vs CCTA alone). Among the 35 patients, stress SPECT-MPI showed myocardial perfusion defects in 37 (35%) vascular territories of the 105 vascular territories in 24 (69%) patients. Vascular territories with a perfusion defect were seen in the LAD (n=14), LCX (n=11) and RCA (n=12). We observed no significant difference in the area under the ROC curve between CCTA plus first-pass CT-MPI and stress SPECT-MPI (0.85 vs 0.78 on a per-vessel basis, respectively, p=0.23, and 0.77 vs 0.70 on a per-patient basis, respectively, p=0.61).

DISCUSSION

The main finding of this study is that first-pass CT-MPI in concert with CCTA significantly improved the area under the ROC curve for distinguishing stenotic coronary arteries compared with CCTA alone in patients without a history of CAD. A decrease in myocardial signal density during diastole suggests that the vascular volume of this myocardium was impaired because of significant stenosis of the epicardial coronary artery. We applied this theory and clearly demonstrated the incremental diagnostic value of first-pass CT-MPI obtained simultaneously with CCTA for assessing significant stenosis of coronary arteries in patients without myocardial infarction.

As intramyocardial perfusion consists mostly of coronary capillaries,[9] stenotic epicardial coronary flow fails to supply optimal coronary blood flow. As a result, capillary resistance increases to maintain capillary hydrostatic pressure, which results in a reduction in myocardial blood volume and perfusion attenuation. Thus, the main reason for impaired blood flow caused by more than 75% stenosis is due to capillary derecruitment rather than the stenosis itself. Several reports have investigated first-pass CT-MPI in a clinical setting. Nagao *et al*[10] showed that first-pass CT-MPI at systole alone shows excellent performance for identifying CAD patients with a sensitivity and specificity of 0.90 and 0.83, respectively, using pharmacological SPECT-MPI as the reference standard. Yoshida *et al*[11] also reported that first-pass CT-MPI alone can detect reduced myocardial enhancement continued from early and late diastole, with a sensitivity and specificity of 0.76 and 0.99, respectively. In the present study we analysed myocardial perfusion during diastole because it is less subject to motion artefacts. The result of the overall diagnostic performance of first-pass CT-MPI in combination with CCTA showed a sensitivity and specificity of 0.85 and 0.94, respectively (per-vessel analysis), which is in line with previous studies. On the other hand, Spiro *et al*[12] reported no significant difference in CT perfusion between patients with or without obstructive CAD. Several reasons for this difference are possible. Regarding technical issues, the timing of the scan with our methods may be later than that in their methods. In our protocol, the delay before the formal scan was calculated as the time to peak enhancement in the ascending aorta plus 3 s to ensure enhancement of the left ventricular myocardium. However, the protocol reported by Spiro *et al* has no delay, which may cause insufficient enhancement, leading to poorer diagnostic accuracy of CT-MPI. Regarding patient characteristics, the body mass index in this study (23±4 kg/m^2) was lower than that in their population (30±8 kg/m^2). Obesity attenuates the X-ray beam, which may make detection of hypoperfusion more difficult.

Our results showed a lower diagnostic accuracy of CCTA than a previous study,[13] especially in terms of the specificity and PPV in both patient-based analysis (0.71) and vessel-based analysis (0.63). This lower diagnostic performance may be explained by high coronary artery calcification in the patients in our study (Agatston score 455 (644), expressed as the median (IQR) in all 145 patients) that may negatively impact CCTA performance; however, the combination of CCTA and CT-MPI significantly improved the diagnostic performance. With per-vessel-based analysis, the specificity increased from 0.87 to 0.94, and PPV increased from 0.63 to 0.79. This diagnostic improvement may be caused by changes in diagnosis with CCTA alone of insufficiently evaluated lesions, which were considered to show significant stenosis owing to severe calcification or substantial banding artefact. Another reason for improvement in the diagnostic performance was due to changes from positive diagnosis in moderate stenotic lesions with CCTA to negative diagnosis with CCTA in combination with CT-MPI. In principle, first-pass CT-MPI showed a defect only with severe stenosis, and first-pass CT-MPI can compensate when CCTA shows borderline stenosis.

First-pass CT-MPI has other advantages. It may provide perfusion information without concerns about adverse reactions to the agents used in pharmacological stress testing. In addition, compared with pharmacological stress CT perfusion, first-pass CT-MPI does not require additional radiation doses or the use

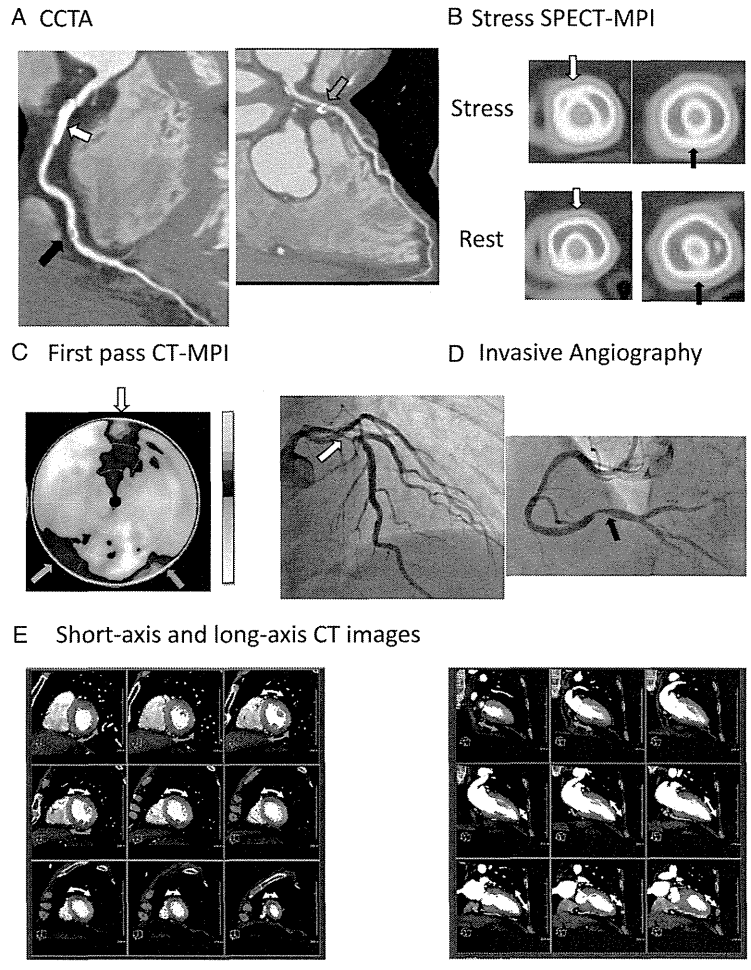

Figure 3 An example of two-vessel disease identified by all modalities. (A) Curved multiplanar reformatted coronary CT angiography (CCTA) image showed a large calcified plaque in the proximal right coronary artery (RCA, white arrow) and significant stenosis in the middle RCA (black arrow). A stenotic lesion was also found in the proximal left anterior descending (LAD) with non-calcified and calcified plaques (red arrow). (B) The single-photon emission CT (SPECT)-myocardial perfusion imaging (MPI) data showed a fully reversible defect throughout the anterior (white arrow) and inferior walls (black arrow). (C) A CT perfusion image showed perfusion defects in the anterior (white arrow), inferoseptum (red arrow) and inferior walls (green arrow). (D) Invasive coronary angiography showed severe stenosis in the proximal LAD (white arrow) and middle of the RCA (black arrow). (E) Short-axial (left) and long-axial (right) left ventricular CT images. Short-axis images show impaired myocardial enhancement throughout the anterior (yellow arrows) and inferior walls (red arrows).

of contrast medium. Thus, first-pass CT-MPI is informative, although it does have some disadvantages. First, CT-MPI shows a potentially high rate of false positives. As first-pass CT-MPI data were obtained at the same time as CCTA, the time gap between attaining images of the epicardial coronary artery and capillary beds is an unsurpassable problem for the first-pass and a one-time image-acquiring protocol. Insufficient filtration of contrast medium into the myocardium may result in false-positive appearances. Second, first-pass CT-MPI cannot distinguish reversible myocardial ischaemia from irreversible myocardial ischaemia. The perfusion defects at the site of an old myocardial infarction are fixed and cannot be distinguished as a defect site that is or is not viable. This study excluded previous myocardial infarction and evidence of Q waves on resting electrocardiography; however, previous cohort studies using cardiac MRI showed the presence of unrecognised myocardial infarction.[14 15] Thus, we cannot deny that a certain number of patients with non-wave myocardial infarction may be included in the current study. Fat deposition in old myocardial infarction and/or decreased vascular blood volume in myocardial scare may substantially alter myocardial signal intensity in the current study. The interpretation of first-pass CT-MPI needs to be made with caution in this issue.

Limitations

There were several limitations in this study. First, this is a single-institution, non-randomised study with a small number of patients. Therefore, further investigations in a larger population are needed to make solid conclusions regarding the value of first-pass CT-MPI. Second, the amount of radiation exposure in this study was relatively high. Our protocol of retrospective gating image acquisition may be an explanation. Our protocol could be improved by using strategies to reduce the radiation dose and electrocardiographically control modulation or prospective sequential scanning.[16] Third, we compared first-pass CT-MPI with stress SPECT-MPI as a non-invasive myocardial perfusion image. However, cardiac MRI may be a better reference standard because SPECT-MPI with poor spatial resolution cannot correctly assess the ischaemic area. Fourth, β-receptor-blocking agents and sublingual nitroglycerin were used before CT data acquisitions in all participants. β-Receptor-blocking agents may have no effect on the perfusion images, but sublingual nitroglycerin may make attenuated perfusion smaller.[17] These medications are generally essential for acquiring evaluable images. Even with these agents, our results demonstrated that first-pass CT-MPI was not inferior to stress SPECT-MPI in this study.

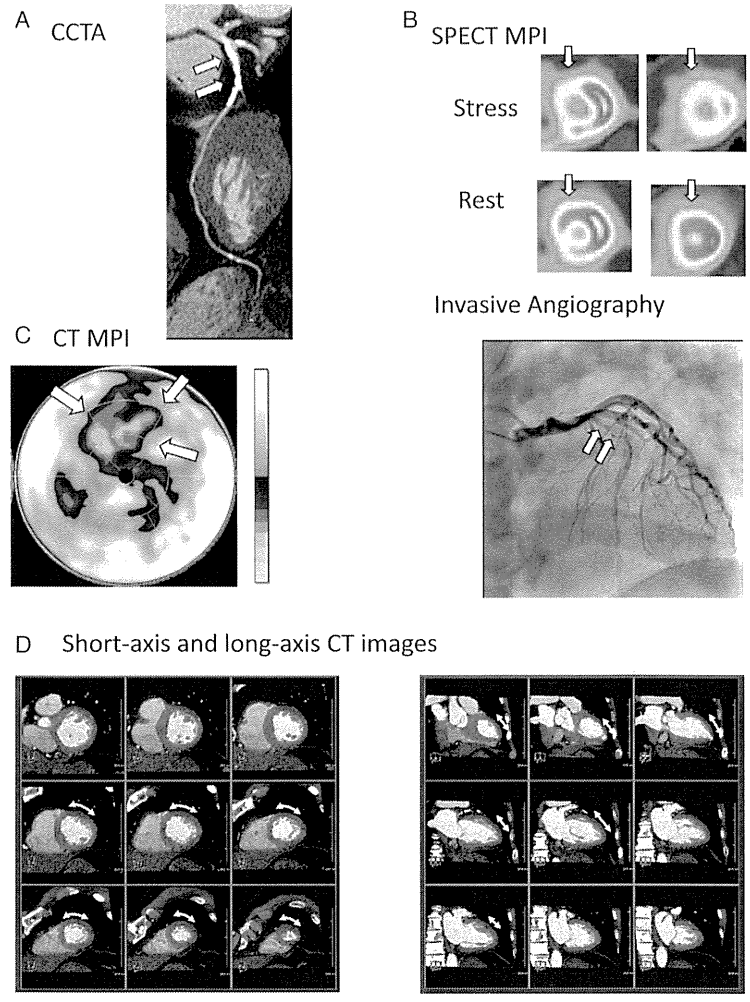

Figure 4 An example of one-vessel disease identified by all modalities. (A) A curved multiplanar reformatted image of coronary CT angiography (CCTA) showed heavy calcification in the proximal portions of the left anterior descending (LAD, white arrows). (B) The single-photon emission CT (SPECT) image showed reversible anterior defects throughout the anterior wall (white arrows). (C) The CT-myocardial perfusion imaging (MPI) data showed a perfusion defect in the anterior wall (white arrows). (D) Invasive coronary angiography showed moderate stenosis in the proximal LAD (white arrows). (E) Short-axial (left) and long-axial (right) left ventricular CT images. Short-axis images show impaired myocardial enhancement in the anterior wall (yellow arrows).

Table 2 Diagnostic accuracy of CCTA, first-pass CT-MPI and CCTA in combination with first-pass CT-MPI for the detection of significantly stenotic coronary arteries in 145 patients

	CCTA		First-pass CT-MPI		CCTA+first-pass CT-MPI	
	Per vessel (n=435)	Per patient (n=145)	Per vessel (n=435)	Per patient (n=145)	Per vessel (n=435)	Per patient (n=145)
No. of results						
True positive	74	46	66	37	77	45
False negative	17	3	25	12	14	4
False positive	44	23	34	11	20	11
True negative	300	73	310	85	324	85
Statistical analysis (%)						
Sensitivity	81	94	73	76	85	92
Specificity	87	76	90	89	94	89
Positive predictive value	63	67	66	77	79	80
Negative predictive value	95	96	93	88	96	96
C statics	0.84 (0.80–0.89)	0.85 (0.80–0.90)	0.81 (0.76–0.86)	0.82 (0.75–0.89)	0.89 (0.86–0.93)	0.90 (0.85–0.95)

CCTA, coronary CT angiography; MPI, myocardial perfusion imaging.

Table 3 Diagnostic accuracy of CCTA, CT-MPI, CCTA in combination with CT-MPI and stress SPECT-MPI for detecting significantly stenotic coronary arteries in 35 patients

	CCTA		First-pass CT-MPI		CCTA+first-pass CT-MPI		Stress SPECT-MPI	
	Per vessel (n=105)	Per patient (n=35)	Per vessel (n=105)	Per patient (n=35)	Per vessel (n=105)	Per patient (n=35)	Per vessel (n=105)	Per patient (n=35)
No. of results								
True positive	33	22	28	18	34	22	28	19
False negative	7	1	12	5	6	1	12	4
False positive	17	8	15	4	20	5	9	5
True negative	48	4	50	8	45	7	56	7
Statistical analysis (%)								
Sensitivity	83	96	70	78	85	96	70	83
Specificity	74	33	77	67	69	58	86	58
Positive predictive value	66	73	65	82	63	81	76	79
Negative predictive value	87	80	81	62	88	88	82	64
C statistic	0.79 (0.72–0.87)	0.65 (0.50–0.79)	0.72 (0.64–0.81)	0.73 (0.56–0.89)	0.85 (0.78–0.920)	0.77 (0.62–0.92)	0.78 (0.70–0.86)	0.71 (0.54–0.871)

CCTA, coronary CT angiography; MPI, myocardial perfusion imaging; SPECT, single-photon emission CT.

CONCLUSIONS

CCTA in combination with first-pass CT-MPI provided excellent diagnostic performance compared with CCTA alone, with invasive coronary angiography as the reference standard in patients without a history of CAD. First-pass CT-MPI makes it possible to evaluate the degree of epicardial coronary stenosis and the extent of impaired myocardium without additional stress, radiation exposure or contrast injection. Thus, first-pass CT-MPI is complementary to CCTA, and the combination of these two diagnostic techniques is feasible in clinical practice.

Key messages

What is already known on this subject?
Pharmacological adenosine stress CT myocardial perfusion imaging is an established method for detecting coronary artery disease. However, the results of studies evaluating the usefulness of first-pass myocardial perfusion imaging without drug loading have not been consistent..

What this study adds?
We evaluated the feasibility and diagnostic accuracy of first-pass myocardial perfusion imaging without drug loading in combination with CT angiography for diagnosing coronary artery disease.

How might this impact on clinical practice?
In this study, first-pass myocardial perfusion imaging in combination with CT angiography significantly improved diagnostic performance compared with CT angiography alone. This technique may complement CT angiography for diagnosing coronary artery disease.

Contributors KO and TM designed the study, drafted the paper, and analysed and interpreted data. YK, KH and SS analysed and interpreted the data. KN, NN and KK designed the study. HM, SK and HI critically revised the manuscript.

Competing interests None.

Patient consent Obtained.

Ethics approval The Ethics Committee of Okayama University Graduate School of Medicine, Dentistry, and Pharmaceutical Sciences.

Provenance and peer review Not commissioned; externally peer reviewed.

REFERENCES

1 Budoff MJ, Dowe D, Jollis JG, *et al*. Diagnostic performance of 64-multidetector row coronary computed tomographic angiography for evaluation of coronary artery stenosis in individuals without known coronary artery disease: results from the prospective multicenter ACCURACY (Assessment by Coronary Computed Tomographic Angiography of Individuals Undergoing Invasive Coronary Angiography) trial. *J Am Coll Cardiol* 2008;52:1724–32.
2 Rozanski A, Gransar H, Hayes SW, *et al*. Temporal trends in the frequency of inducible myocardial ischemia during cardiac stress testing: 1991 to 2009. *J Am Coll Cardiol* 2013;61:1054–65.
3 Porter TR, Smith LM, Wu J, *et al*. Patient outcome following 2 different stress imaging approaches: a prospective randomized comparison. *J Am Coll Cardiol* 2013;61:2446–55.
4 Bettencourt N, Chiribiri A, Schuster A, *et al*. Direct comparison of cardiac magnetic resonance and multidetector computed tomography stress-rest perfusion imaging for detection of coronary artery disease. *J Am Coll Cardiol* 2013;61:1099–107.
5 George RT, Arbab-Zadeh A, Miller JM, *et al*. Adenosine stress 64- and 256-row detector computed tomography angiography and perfusion imaging: a pilot study evaluating the transmural extent of perfusion abnormalities to predict atherosclerosis causing myocardial ischemia. *Circ Cardiovasc Imaging* 2009;2:174–82.
6 Jayaweera AR, Wei K, Coggins M, *et al*. Role of capillaries in determining CBF reserve: new insights using myocardial contrast echocardiography. *Am J Physiol* 1999;277:H2363–72.
7 Lindner JR, Skyba DM, Goodman NC, *et al*. Changes in myocardial blood volume with graded coronary stenosis. *Am J Physiol* 1997;272:H567–75.
8 Osawa K, Miyoshi T, Sato S, *et al*. Safety and efficacy of a bolus injection of landiolol hydrochloride as a premedication for multidetector-row computed tomography coronary angiography. *Circ J* 2012;77:146–52.
9 Cerqueira MD, Weissman NJ, Dilsizian V, *et al*. Standardized myocardial segmentation and nomenclature for tomographic imaging of the heart. A statement for healthcare professionals from the Cardiac Imaging Committee of the Council on Clinical Cardiology of the American Heart Association. *Int J Cardiovasc Imaging* 2002;18:539–42.
10 Nagao M, Matsuoka H, Kawakami H, *et al*. Detection of myocardial ischemia using 64-slice MDCT. *Circ J* 2009;73:905–11.
11 Yoshida K, Shimada K, Tanaka A, *et al*. Quantitative analysis of myocardial contrast enhancement by first-pass 64-multidetector computed tomography in patients with coronary heart disease. *Circ J* 2009;73:116–24.
12 Spiro AJ, Haramati LB, Jain VR, *et al*. Resting cardiac 64-MDCT does not reliably detect myocardial ischemia identified by radionuclide imaging. *AJR Am J Roentgenol* 2013;200:337–42.

13 Guo SL, Guo YM, Zhai YN, *et al*. Diagnostic accuracy of first generation dual-source computed tomography in the assessment of coronary artery disease: a meta-analysis from 24 studies. *Int J Cardiovasc Imaging* 2011;27: 755–71.
14 Kwong RY, Sattar H, Wu H, *et al*. Incidence and prognostic implication of unrecognized myocardial scar characterized by cardiac magnetic resonance in diabetic patients without clinical evidence of myocardial infarction. *Circulation* 2008;118:1011–20.
15 Schelbert EB, Cao JJ, Sigurdsson S, *et al*. Prevalence and prognosis of unrecognized myocardial infarction determined by cardiac magnetic resonance in older adults. *JAMA* 2012;308:890–6.
16 Hausleiter J, Meyer T, Hadamitzky M, *et al*. Radiation dose estimates from cardiac multislice computed tomography in daily practice: impact of different scanning protocols on effective dose estimates. *Circulation* 2006;113:1305–10.
17 Techasith T, Cury RC. Stress myocardial CT perfusion: an update and future perspective. *JACC Cardiovasc Imaging* 2011;4:905–16.

Heart

Additional diagnostic value of first-pass myocardial perfusion imaging without stress when combined with 64-row detector coronary CT angiography in patients with coronary artery disease

Kazuhiro Osawa, Toru Miyoshi, Yasushi Koyama, Katsushi Hashimoto, Shuhei Sato, Kazufumi Nakamura, Nobuhiro Nishii, Kunihisa Kohno, Hiroshi Morita, Susumu Kanazawa and Hiroshi Ito

Heart 2014 100: 1008-1015 originally published online April 24, 2014
doi: 10.1136/heartjnl-2013-305468

American Journal of Internal Medicine
2014; 2(4): 79-82
Published online August 10, 2014 (http://www.sciencepublishinggroup.com/j/ajim)
doi: 10.11648/j.ajim.20140204.15
ISSN: 2330-4316 (Print); ISSN: 2330-4324 (Online)

An autopsic examination case of diagnosed Brugada syndrome

Satoshi Furukawa[1, 4], Satomu Morita[1], Hayato Okunaga[1], Lisa Wingenfeld[1], Akari Takaya[1], Tokiko Nakagawa[1], Ikuo Sakaguchi[1], Yoshio Yamamoto[2], Takasi Ashihara[3], Minoru Horie[3], Katsuji Nishi[3], Masahito Hitosugi[1]

[1]Department of Legal Medicine, Shiga University of Medical Science, Shiga, Japan
[2]Iga Research Institute of Mie University, Mie, Japan
[3]Department of Cardiovascular and Respiratory Medicine, Shiga University of Medical Science, Shiga, Japan
[4]Department of Legal Medicine, Shiga University of Medical Science, Setatsukinowa, Otsu City, Shiga 520-2192, Japan

Email address:
31041220@belle.shiga-med.ac.jp (S. Furukawa)

To cite this article:
Satoshi Furukawa, Satomu Morita, Hayato Okunaga, Lisa Wingenfeld, Akari Takaya, Tokiko Nakagawa, Ikuo Sakaguchi, Yoshio Yamamoto, Takasi Ashihara, Minoru Horie, Katsuji Nishi, Masahito Hitosugi. An Autopsic Examination Case of Diagnosed Brugada Syndrome. *American Journal of Internal Medicine.* Vol. 2, No. 4, 2014, pp. 79-82. doi: 10.11648/j.ajim.20140204.15

Abstract: Brugada syndrome is a cardiac disorder characterized by typical ECG alterations, and it is associated with a high risk for sudden cardiac death, affecting young subjects with structurally normal hearts. The prevalence of this disorder is still uncertain, presenting marked geographical differences. The syndrome has a genetic basis, and several mutations have been identified in genes encoding subunits of cardiac sodium, potassium, and calcium channels, as well as in genes involved in the trafficking or regulation of these channels. We experienced an autopsy case of the sudden death by diagnosed Brugada syndrome. We present the case report and autopsic findings.

Keywords: Brugada Syndrome, Sudden Death, Coved and Saddleback Type ST Elevation, Autopsy, Histological Findings

1. Introduction

Brugada syndrome (BS) has originally been described as an autosomal-dominant inherited arrhythmic disorder characterized by ST elevation with successive negative T wave in the right precordial leads without structural cardiac abnormalities [1.2]. Patients are at risk for sudden cardiac death (SCD) due to ventricular fibrillation (VF). Since 1953, the ECG pattern similar to coved-type ST-segment elevation was reported as a normal variant in the healthy population or related to VF with structural abnormality [3-5]. BS is a genetically determined disease, characterized by typical electrocardiographic signs, and it predisposes to sudden cardiac death (SCD) secondary to polymorphic ventricular tachycardia (PVT)/ventricular fibrillation (VF) in the absence of structural heart disease. It was first described in 1992 by Pedro and Josep Brugada [1]. Brugada and Brugada linked an abnormal ECG with right bundle branch block pattern and coved-type ST elevation over the right precordial leads to primary ventricular fibrillation (VF) and sudden cardiac death (SCD) in patients with structurally normal hearts [1]. It instantly became known as Brugada syndrome (BS) and has drawn the worldwide attention of cardiologists, electrophysiologists and molecular biologists/geneticists. We present an autopsy case of diagnosed BS.

2. Case Report

A 33-year-old man was found lying on the floor in his house. He had pointed the electrocardiogram (ECG) abnormality five years before in the medical examination. The ECG showed the coved and saddleback type ST elevation in leads V1 through V3. (Figure.1) His mother was dead of unknown origin in her thirties. The ECG classified the Brugada pattern and he diagnosed Brugada syndrome.

The autopsy was performed on the day following death. The body was 162 cm in height and 63.8 kg in weight. Postmortem lividity was large in his back. A large number of

petechiea in the conjunctiva was also recognized. (Figure.2) The heart weighed 297.7g.

Autopsy findings revealed that the intevals of cardiac cells were wide to each other, and there were inflammation, small hemorrhage and fibrosis in the right ventricle especially. (Figure. 3-6)

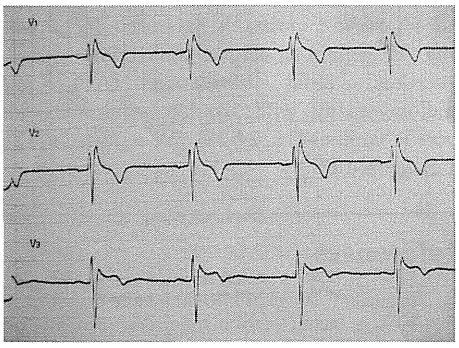

Figure 1. *Brugada syndrome ECG pattern with coved-type pattern (Type 1) in leads $V_{1,2}$ and saddleback-type pattern (Type 2) in leads V_3.*

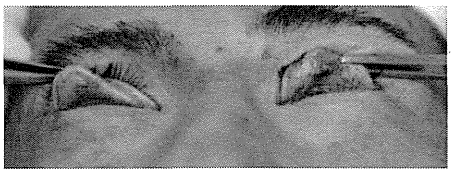

Figure 2. *A large number of petechiea in the conjunctiva.*

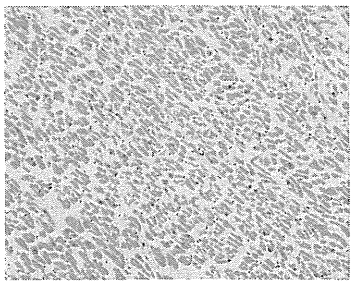

Figure 3. *The intervals of cardiac cells were wide to each other in the right ventricle. (magnification×400)*

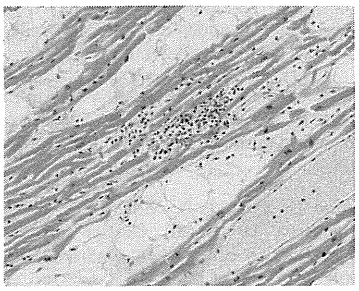

Figure 4. *The inflammation and fibrosis in cardiac muscle. The small hemorrhage in the adipose tissue. (the right ventricle) (magnification×400)*

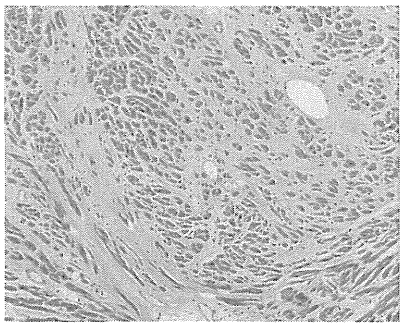

Figure 5. *The inflammation and fibrosis in cardiac muscle. The small hemorrhage in the adipose tissue. (the right ventricle) (magnification×400)*

Figure 6. *The inflammation and fibrosis in cardiac muscle. The small hemorrhage in the adipose tissue. (the right ventricle) (magnification×400)*

3. Discussion

The clinical spectrum of the BS patient ranges from asymptomatic to SCD [6].

Patients may have a late onset of VF, despite having had an abnormal ECG pattern for decades [6.7]. Syncope or seizures because of self-terminating VF episodes are also common, as are agonal respiration and difficulty in arousal at night, again caused by self-terminating VF episodes [6.7]. The majority of BS patients are relatively young, between 20 and 40 years of age, but the youngest patient diagnosed with the syndrome was 2 days old and the oldest 84 years [6.8]. Despite an autosomal dominant inheritance pattern, BS prevalence is up to 10-fold higher in males and with greater severity [7.9]. Worldwide, the syndrome is probably responsible for 4-12% of all sudden deaths and at least 20% of sudden deaths in patients with structurally normal hearts [2.6]. There is also a difference between the incidence of the Brugada type 1 ECG pattern and the syndrome itself, as defined by the 2005 Consensus criteria. Miyasaka et al observed a type 1 Brugada ECG pattern in 12 per 10,000 inhabitants; type 2 and 3 ECGs were more prevalent, appearing in 58 per 10,000 inhabitants [10]. The prevalence of a Brugada ECG is higher in Asia (0.36%) and Europe (0.25%) than in the USA (0.03%) [11]. However, the true prevalence of BS is unknown because the ECG pattern can be wax and wane, making it very likely that the true incidence is underestimated.

Table 1. Three types of Brugada ECG patterns.

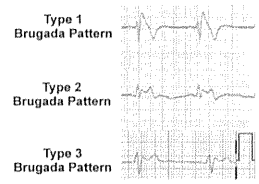

Type 1 is a coved-type pattern and type 2 is a saddleback-type, which has ST elevation ≥2 mm without T-wave inversion. Type 3 pattern shows a J-point elevation without ST elevation ≥1 mm.

The diagnostic criteria of BS consist of 2 parts: (1) detection of the typical ECG abnormality and (2) clinical characteristics [6]. The 2 Brugada consensus reports classified the Brugada ECG pattern into 3 types (Table.1): (1) type 1 pattern has ST elevation ≥2 mm, giving rise to a coved-type ST-segment, in electrical continuity with a negative T-wave and without a separating isoelectric; (2) type 2 has a high take-off ST-segment elevation. In this variant, the J-point elevation (≥2 mm) gives rise to a gradually descending elevated ST-segment (remaining >1mm above the baseline) and a positive or biphasic T- wave. This ST-T segment morphology is referred to as the saddleback type; (3) type 3 is the coved- or saddleback-type with <1mm ST-elevation ST-segment elevation [2.6]. In conjunction with the ECG abnormality, 1 of the following criteria is necessary: (1) a history of VT/VF, (2) a family history of SCD, (3) a family history of coved-type ECG, (4) agonal respiration during sleep, or (5) inducibility of VT/VF during electrophysiological study. Importantly, the aforementioned criteria have not been proven to be good risk factors, except for a history of VT/VF.

In recent years, it has become clear that the right ventricular outflow tract (RVOT) is the likely arrhythmogenic substrate site, and the RVOT is the only cardiac structure lying just beneath the second and third intercostal spaces. The consensus reports recommend the following clinical manifestations: (1) history of spontaneous VT/VF episode or aborted SCD; (2) family history of SCD or coved-type ECG; (3) agonal respiration during sleep; or (4) inducibility of VT/VF by programmed electrical stimulation (PES). In 1998, Chen et al reported the first mutation, linked to BS, in the *SCN5A* gene, which encodes for the α-subunit of the sodium channel [12]. Since then, there have been an increasing number of gene mutations identified [6.11.13].

Functional studies demonstrate that *SCN5A* mutations in BS patients cause loss of function of the sodium channel because of decreased expression of the sodium channel protein, sarcolemma, expression of non-functional channels or altered gating properties (delayed activation, earlier inactivation, faster inactivation, enhanced slow inactivation and delayed recovery from inactivation) [14-20]. The loss of function of the sodium channel results in a decrease in the sodium current, which in turn impairs the fast upstroke of phase 0 of the action potential (AP), causing slow conduction in the heart.

Even though *SCN5A* mutations are the most common type found in 11–28% of BS probands, the genetics of BS have be- come heterogeneous. In addition to the *SCN5A* mutations, more mutations are found in the gene encoding the proteins of the potassium and calcium channels. *SCN5A* mutations may cause not only BS but other diseases as well. Indeed, *SCN5A* mutations have also been associated with long QT syndrome, cardiac conduction disease, sick sinus syndrome, atrial fibrillation (AF), and dilated cardiomyopathy with overlap syndromes identified in specific families [16. 21-25]. We reported the autopsy case of diagnosed BS.

References

[1] Brugada P, Brugada J. Right bundle branch block, persistent ST seg- ment elevation and sudden cardiac death: a distinct clinical and elec- trocardiographic syndrome. A multicenter report. J Am Coll Cardiol. 1992;20: 1391–1396.

[2] Wilde AA, Antzelevitch C, Borggrefe M, Brugada J, Brugada R, Brugada P, Corrado D, Hauer RN, Kass RS, Nademanee K, Priori SG, Towbin JA. Proposed diagnostic criteria for the Brugada syndrome: consensus report. Circulation. 2002; 106: 2514–2519.

[3] Osher HL, Wolff L. Electrocardiographic pattern simulating acute myo- cardial injury. Am J Med Sci. 1953; 226:541–545.

[4] Edeiken J. Elevation of the RS-T segment, apparent or real, in the right precordial leads as a probable normal variant. Am Heart J. 1954; 48:331–339.

[5] Martini B, Nava A, Thiene G, Buja GF, Canciani B, Scognamiglio R, Daliento L, Dalla VS. Ventricular fibrillation without apparent heart dis- ease: description of six cases. Am Heart J. 1989;118:1203–1209.

[6] Antzelevitch C, Brugada P, Borggrefe M, Brugada J, Brugada R, Corrado D, et al. Brugada syndrome: Report of the second consensus conference: Endorsed by the Heart Rhythm Society and the European Heart Rhythm Association. Circulation 2005; 111: 659 – 670.

[7] Nademanee K, Veerakul G, Nimmannit S, Chaowakul V, Bhuripanyo K, Likittanasombat K, et al. Arrhythmogenic marker for the sudden unexplained death syndrome in Thai men. Circulation 1997; 96: 2595 – 2600.

[8] Probst V, Denjoy I, Meregalli PG, Amirault JC, Sacher F, Mansourati J, et al. Clinical aspects and prognosis of Brugada syndrome in children. Circulation 2007; 115: 2042 – 2048.

[9] Benito B, Sarkozy A, Mont L, Henkens S, Berruezo A, Tamborero D, et al. Gender differences in clinical manifestations of Brugada syndrome. J Am Coll Cardiol 2008; 52: 1567 – 1573.

[10] Miyasaka Y, Tsuji H, Yamada K, Tokunaga S, Saito D, Imuro Y, et al. Prevalence and mortality of the Brugada-type electrocardio- gram in one city in Japan. J Am Coll Cardiol 2001; 38: 771 – 774.

[11] Mizusawa Y, Wilde A. Brugada syndrome. Circ Arrhythm Electro- physiol 2012; 5: 606 – 616.

[12] Chen Q, Kirsch GE, Zhang D, Brugada R, Brugada J, Brugada P. et al. Genetic basis and molecular mechanism for idiopathic ven- tricular fibrillation. Nature 1998; 392: 293 – 296.

[13] Priori SG, Napolitano C, Giordano U, Collisani G, Memmi M. Brugada syndrome and sudden cardiac death in children. Lancet 2000; 355: 808 – 809.

[14] Valdivia CR, Tester DJ, Rok BA, Porter CB, Munger TM, Jahangir A, et al. A trafficking defective, Brugada syndrome-causing SCN5A. mutation rescued by drugs. Cardiovasc Res 2004; 62: 53 – 62.

[15] Kyndt F, Probst V, Potet F, Demolombe S, Chevallier JC, Baro I, et al. Novel SCN5A mutation leading either to isolated cardiac. conduction defect or Brugada syndrome in a large French family. Circulation 2001; 104: 3081 – 3086.

[16] Bezzina C, Veldkamp MW, van den Berg MP, Postma AV, Rook MB, Viersma JW, et al. A single Na(+) channel mutation causing. both long-QT and Brugada syndromes. Circ Res 1999; 85: 1206 – 1213.

[17] Dumaine R, Towbin JA, Brugada P, Vatta M, Nesterenko DV, Nesterenko VV, et al. Ionic mechanisms responsible for the elec- trocardiographic phenotype of the Brugada syndrome are temperature dependent. Circ Res 1999; 85: 803 – 809.

[18] Akai J, Makita N, Sakurada H, Shirai N, Ueda K, Kitabatake A, et al. A novel SCN5A mutation associated with idiopathic ventricular. fibrillation without typical ECG findings of Brugada syndrome. FEBS Lett 2000; 479: 29 – 34.

[19] Amin AS, Verkerk AO, Bhuiyan ZA, Wilde AA, Tan HL. Novel. Brugada syndrome-causing mutation in ion-conducting pore of cardiac Na+ channel does not affect ion selectivity properties. Acta Physiol Scand 2005; 185: 291 – 301.

[20] Lei M, Huang CL, Zhang Y. Genetic Na+ channelopathies and sinus node dysfunction. Prog Biophys Mol Biol 2008; 98: 171 – 178.

[21] Wang Q, Shen J, Splawski I, Atkinson D, Li Z, Robinson JL, et al. SCN5A mutations associated with an inherited cardiac arrhythmia, long QT syndrome. Cell 1995; 80: 805 – 811.

[22] Tan HL, Bink-Boelkens MT, Bezzina CR, Viswnathan PC, Beaufort- Krol GC, van Tintelen PJ, et al. A sodium-channel mutation causes isolated cardiac conduction disease. Nature 2001; 409: 1043 – 1047.

[23] Benson DW, Wang DW, Dyment M, Knilans TK, Fish FA, Strieper MJ, et al. Congenital sick sinus syndrome caused by recessive muta- tions in the cardiac sodium channel gene (SCN5A). J Clin Invest 2003; 112: 1019 – 1028.

[24] Darbar D, Kannankeril PJ, Donahue BS, Kucera G, Stubblefield T, Haines JL, et al. Cardiac sodium channel (SCN5A) variants associated with atrial fibrillation. Circulation 2008; 117: 1927 – 1935.

[25] Olson TM, Michels VV, Ballew JD, Reyna SP, Karst ML, Herron KJ, et al. Sodium channel mutations and susceptibility to heart failure and atrial fibrillation. JAMA 2005, 293: 447 – 454.

International Journal of Cardiology 172 (2014) e111–e113

Contents lists available at ScienceDirect

International Journal of Cardiology

journal homepage: www.elsevier.com/locate/ijcard

Letter to the Editor

Augmentation of the J wave by rapid pacing in a patient with vasospastic angina

Akinori Sato [a,*], Hiroshi Watanabe [a], Keiko Sonoda [a], Masaomi Chinushi [b], Takashi Tsuda [c], Daisuke Izumi [a], Hiroshi Furushima [a], Tohru Minamino [a]

[a] Department of Cardiovascular Biology and Medicine, Graduate School of Medical and Dental Sciences, Niigata University, Niigata, Japan
[b] Graduate School of Health Sciences, Niigata University School of Medicine, Niigata, Japan
[c] Kido Hospital, Niigata, Japan

ARTICLE INFO

Article history:
Received 1 October 2013
Accepted 22 December 2013
Available online 4 January 2014

Keywords:
J wave
Early repolarization syndrome
Vasospastic angina
Myocardial ischemia
Pacing rate

Early repolarization or a J wave, which is a notch or slur at the terminal part of the QRS complex with or without ST-segment elevation on an electrocardiogram (ECG), is common in healthy individuals and has been considered benign for decades. However, early repolarization in the inferior and/or lateral leads has recently been associated with ventricular fibrillation (VF) and sudden cardiac death, particularly in subjects without structural heart abnormalities, and early repolarization syndrome was proposed as a new arrhythmia disease [1]. Furthermore, early repolarization has been associated with structural heart diseases including acute myocardial infarction and vasospastic angina [2,3]. The amplitude of the J wave is affected by various conditions such as body temperature, heart rate, and autonomous nerve activity and usually increases during slow heart rate in patients with early repolarization syndrome [4,5], but the precise mechanisms remain unclear. Here, we describe a case of vasospastic angina and slight myocardial damage, in which J waves were augmented by ischemia during coronary vasospasm and by increasing atrial pacing rate.

A 64-year-old male was admitted to our hospital due to a first episode of syncope, which occurred at rest after lunch with no preceding symptoms. His physical examination, brain magnetic resonance imaging (MRI), and echocardiography were normal. The ECG showed distinct J waves in the inferior leads (Fig. 1A). The signal-averaged ECG did not reveal late potentials, and the head-up tilt test was negative. A left ventriculography showed slight inferoposterior dyskinesia, but coronary angiography did not show significant stenosis (Fig. 1E). Injection of 10 mg ergonovine into the right coronary artery induced spastic occlusion (Fig. 1F) and caused augmentation of the J waves with ST-segment depression and subsequent ST-segment elevation in the inferior leads (Fig. 1B and C). The patient remained hemodynamically stable during the induced spasm, and ventricular tachyarrhythmias did not occur. After spasm was relieved with intracoronary isosorbide dinitrate, the amplitude of the J waves returned to the baseline level. Cardiac magnetic resonance imaging showed subendocardial delayed-gadolinium enhancement at the basal inferoposterior wall of left ventricle (Fig. 1G and H).

We studied the heart rate-dependent change in the J wave during an electrophysiological study. J-wave amplitude was augmented as atrial pacing rate was increased (Fig. 2A). Wenckebach type atrioventricular block was observed during an atrial pacing rate of 120 bpm. Similarly, progressive shortening of the extra-stimuli coupling interval resulted in a gradual increase in J-wave amplitude (Fig. 2B and C). Furthermore, the J wave was attenuated after pauses following the extra-stimuli (Fig. 2B and C). No sustained ventricular tachyarrhythmia was induced by up to three extra-stimuli from two sites of the right ventricle and one site of the left ventricle. Intravenous administration of the Na^+ channel blocker pilsicainide (1 mg/kg) resulted in fragmentation of the QRS complex and further isolation of the J waves from QRS complexes in the inferior leads (Fig. 1D). Ca^{2+} channel blocker (benidipine and diltiazem) treatment was initiated for vasospastic angina, and no cardiac event occurred during a 3-year follow-up.

Although the underlying pathophysiological mechanisms of J wave syndrome are unclear, there are the two leading hypotheses for Brugada syndrome, a form of J wave syndrome [6–8]. Findings from both experimental models and humans support a "repolarization hypothesis" that J waves represent transmural differences in the action potential at the early repolarization phase [7]. However, the "depolarization hypothesis" relies on structural abnormalities including fatty replacement and fibrosis and on slowing of electrical pulse conduction [6,8]. A similar controversy about the mechanisms exists for early repolarization syndrome, another form of J wave syndrome proposed recently [5,9]. In an

* Corresponding author at: Department of Cardiovascular Biology and Medicine, Graduate School of Medical and Dental Sciences, Niigata University, 1-757 Asahimachi Chuou-ku, Niigata, 951-8510, Japan. Tel.: +81 25 227 2185; fax: +81 25 227 0774.
E-mail address: akinosatou-circ@umin.ac.jp (A. Sato).

0167-5273/$ – see front matter
http://dx.doi.org/10.1016/j.ijcard.2013.12.121

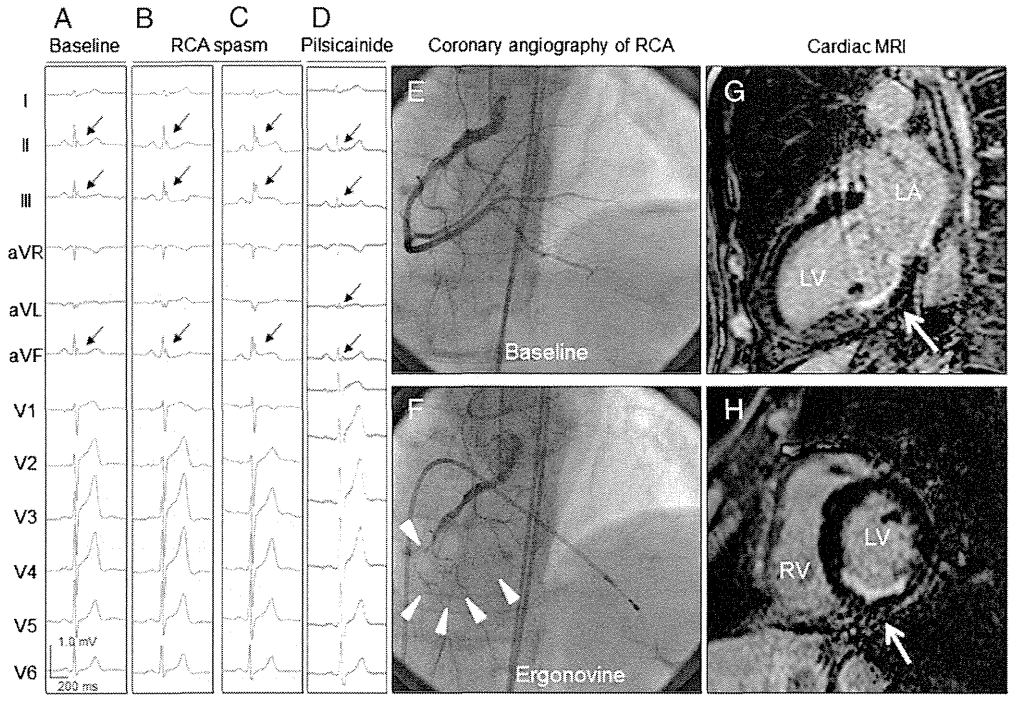

Fig. 1. A. Baseline electrocardiogram showing notch-type J waves in the inferior leads (arrows). B and C. After the ergonovine-induced vasospasm of the right coronary artery (RCA), the J waves were progressively augmented with an ST-segment depression and subsequent ST-segment elevation. D. Intravenous administration of pilsicainide caused fragmentation of the QRS complex and further isolation of the J wave from the QRS complex in the inferior and aVL leads. E, Baseline coronary angiogram showing a normal RCA. F. Intracoronary injection of ergonovine provoked a vasospasm in the middle portion of the RCA, resulting in its total occlusion (arrowheads). G and H. Cardiac magnetic resonance imaging (MRI) revealed delayed-gadolinium enhancement in the subendocardium of the basal inferoposterior left ventricular wall (arrows). LA, left atrium; LV, left ventricle; RV, right ventricle.

experimental model, transmural dispersion of the action potential results in early repolarization pattern [5]. However, we have recently found that slow conduction and structural abnormalities exist in patients with early repolarization syndrome [9]. Although pause-dependent augmentation of J waves has been reported recently [4], our case showed the opposite phenomenon in that J wave amplitude was augmented as pacing rate was increased and was attenuated after a pause, suggesting that conduction velocity of the ventricular myocardium plays an important role in the J wave. Our hypothesis is supported by the finding that the J wave was isolated from the QRS complex by administration of a Na^+ channel blocker, which reduces myocardial conduction velocity and that the area of myocardial damage (inferoposterior wall) was consistent with the electrocardiogram leads where J waves manifest.

Our case also showed ischemia-induced augmentation of J waves. Increasing evidence suggests that the J wave is associated with ischemic heart disease [2,3]. The presence of a J wave is a predictor of the development of ventricular fibrillation during acute myocardial ischemia [2]. In our prior study, the J wave was augmented by myocardial ischemia during coronary spasms, and the presence and augmentation of J waves, particularly prominent J waves with the characteristic ST-elevation patterns, were associated with ventricular fibrillation during spasms [3].

In conclusion, our case showed two unique characteristics of J waves: rate-dependent augmentation and ischemia-induced augmentation. Various pathophysiological mechanisms may underlie J wave syndrome, as there are multiple causative genes [10].

References

[1] Haissaguerre M, Derval N, Sacher F, et al. Sudden cardiac arrest associated with early repolarization. N Engl J Med 2008;358:2016–23.
[2] Tikkanen JT, Wichmann V, Junttila MJ, et al. Association of early repolarization and sudden cardiac death during an acute coronary event. Circ Arrhythm Electrophysiol 2012;5:714–8.
[3] Sato A, Tanabe Y, Chinushi M, et al. Analysis of J waves during myocardial ischaemia. Europace 2011;14:715–23.
[4] Aizawa Y, Sato A, Watanabe H, et al. Dynamicity of the J-wave in idiopathic ventricular fibrillation with a special reference to pause-dependent augmentation of the J-wave. J Am Coll Cardiol 2012;59:1948–53.
[5] Yan GX, Antzelevitch C. Cellular basis for the electrocardiographic J wave. Circulation 1996;93:372–9.
[6] Coronel R, Casini S, Koopmann TT, et al. Right ventricular fibrosis and conduction delay in a patient with clinical signs of Brugada syndrome: a combined electrophysiological, genetic, histopathologic, and computational study. Circulation 2005;112:2769–77.
[7] Kurita T, Shimizu W, Inagaki M, et al. The electrophysiologic mechanism of ST-segment elevation in Brugada syndrome. J Am Coll Cardiol 2002;40:330–4.
[8] Zumhagen S, Spieker T, Rolinck J, et al. Absence of pathognomonic or inflammatory patterns in cardiac biopsies from patients with Brugada syndrome. Circ Arrhythm Electrophysiol 2009;2:16–23.
[9] Watanabe H, Ohkubo K, Watanabe I, et al. SCN5A mutation associated with ventricular fibrillation, early repolarization, and concealed myocardial abnormalities. Int J Cardiol 2013;165:e21–3.
[10] Antzelevitch C. Genetic, molecular and cellular mechanisms underlying the J wave syndromes. Circ J 2012;76:1054–65.

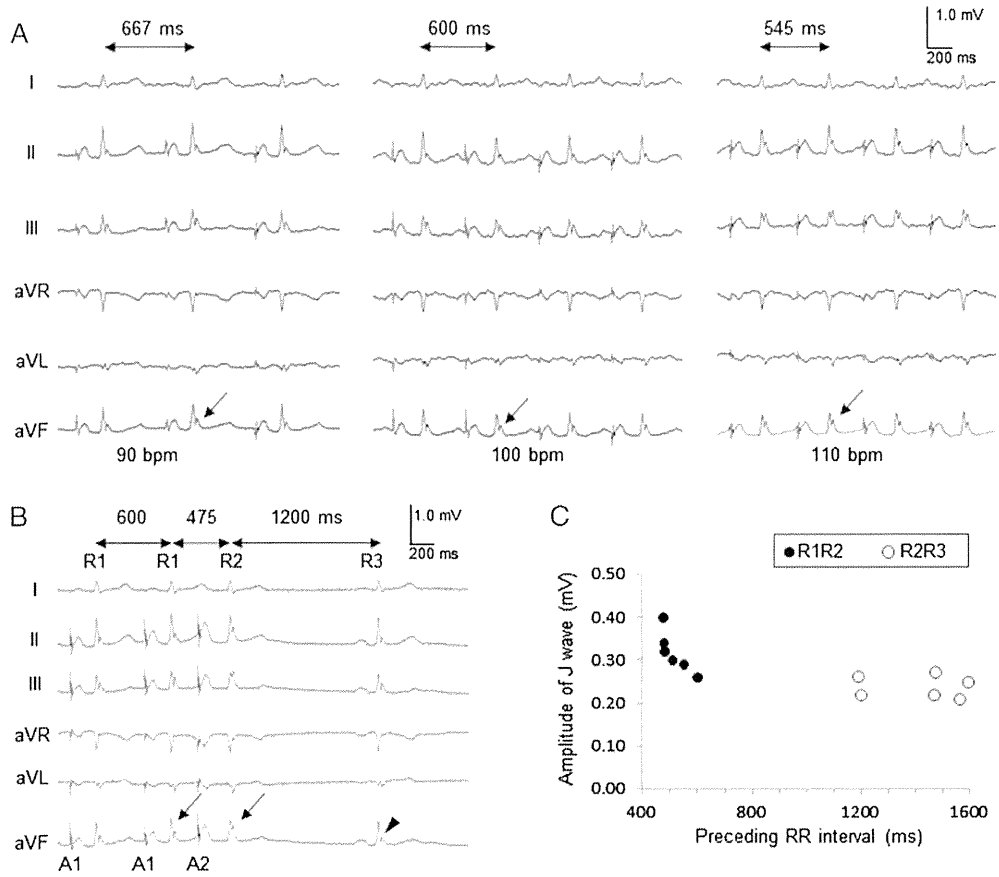

Fig. 2. A. J-wave amplitude was augmented as atrial pacing rate was increased (90, 100, and 110 bpm) (arrows). B. J-wave amplitude was augmented after extra-stimulation (arrows). Pause after extra-stimulation resulted in attenuation of the J wave (arrowhead). C. Relationship between J-wave amplitude in lead aVF and the preceding RR interval during single atrial extrastimulation (R1R2) or the pause-interval after extra-stimulation (R2R3). J-wave amplitude was augmented as R1R2 decreased, whereas it was attenuated after the pause-interval.

Cardiac Channelopathies Associated with Infantile Fatal Ventricular Arrhythmias: From the Cradle to the Bench

KOICHI KATO, M.D.,* TAKERU MAKIYAMA, M.D., PH.D.,† JIE WU, PH.D.,*,‡ WEI-GUANG DING, PH.D.,§ HIROMI KIMURA, M.D., PH.D.,* NOBU NAIKI, M.D.,* SEIKO OHNO, M.D., PH.D.,* HIDEKI ITOH, M.D., PH.D.,* TOSHIO NAKANISHI, M.D., PH.D.,¶ HIROSHI MATSUURA, M.D., PH.D.,§ and MINORU HORIE, M.D., PH.D.*

From the *Department of Cardiovascular and Respiratory Medicine, Shiga University of Medical Science, Shiga, Japan; †Department of Cardiovascular Medicine, Kyoto University Graduate School of Medicine, Kyoto, Japan; ‡Department of Pharmacology, Medical School of Xi'an Jiaotong University, Xi'an, China; §Department of Physiology, Shiga University of Medical Science, Shiga, Japan; and ¶Department of Pediatric Cardiology, Tokyo Women's Medical University, Tokyo, Japan

Channelopathies in Infantile Arrhythmias. ***Background:*** **Fatal ventricular arrhythmias in the early period of life have been associated with cardiac channelopathies for decades, and postmortem analyses in SIDS victims have provided evidence of this association. However, the prevalence and functional properties of cardiac ion channel mutations in infantile fatal arrhythmia cases are not clear.**

Methods and Results: **Seven infants with potentially lethal arrhythmias at age < 1 year (5 males, age of onset 44.1 ± 72.1 days) were genetically analyzed for *KCNQ1, KCNH2, KCNE1–5, KCNJ2, SCN5A, GJA5,* and *CALM1* by using denaturing high-performance liquid chromatography and direct sequencing. Whole-cell currents of wildtype and mutant channels were recorded and analyzed in Chinese hamster ovary cells transfected with *SCN5A* and *KCNH2* cDNA. In 5 of 7 patients, we identified 4 mutations (p.N1774D, p.T290fsX53, p.F1486del and p.N406K) in *SCN5A*, and 1 mutation (p.G628D) in *KCNH2*. N1774D, F1486del, and N406K in *SCN5A* displayed tetrodotoxin-sensitive persistent late Na^+ currents. By contrast, *SCN5A*-T290fsX53 was nonfunctional. *KCNH2*-G628D exhibited loss of channel function.**

Conclusion: **Genetic screening of 7 patients was used to demonstrate the high prevalence of cardiac channelopathies. Functional assays revealed both gain and loss of channel function in *SCN5A* mutations, as well as loss of function associated with the *KCNH2* mutation.** *(J Cardiovasc Electrophysiol, Vol. 25, pp. 66-73, January 2014)*

Brugada syndrome, long-QT syndrome, KCNH2, SCN5A, SIDS, ventricular arrhythmia

Introduction

Long-QT syndrome (LQTS)[1,2] and Brugada syndrome (BrS)[3,4] are inherited diseases characterized by a high incidence of ventricular arrhythmia attacks and consequent sudden death. The recent identification of responsible mutations in cardiac ion channel genes has led to the classification of these clinical entities as "channelopathies."

Fatal ventricular arrhythmias in the early period of life are fairly rare events. Channelopathies were first associated with these events more than a decade ago,[5] and postmortem analyses of victims of sudden infant death syndrome (SIDS)[6-8] have indirectly supported this hypothesis.[9-14] In recent studies, high prevalence of sodium channel mutations among these patients has been suspected;[9,15] however, the actual prevalence of channelopathies in infantile fatal arrhythmia patients is not clear because of the lack of clinical information. In this study, we surveyed 7 Japanese infants with a history of fatal ventricular arrhythmias at < 1 year of age, to elucidate the underlying mechanism.

Drs. Kato and Makiyama contributed equally to this work.

This work was supported by research grants from the Ministry of Education, Culture, Science, and Technology of Japan, health science research grants from the Ministry of Health, Labor and Welfare of Japan for Clinical Research on Measures for Intractable Diseases, the Translational Research Funds from the Japan Circulation Society (to MH), and a grant from the National Natural Science Foundation of China (#81273501 to JW).

No disclosures.

Address for correspondence: Minoru Horie, M.D., PH.D., Department of Cardiovascular and Respiratory Medicine, Shiga University of Medical Science, Seta-Tsukinowa, Otsu, Shiga, Japan, 520-2192. Fax: +81-77-543-5839; E-mail: horie@belle.shiga-med.ac.jp

Manuscript received 2 May 2013; Revised manuscript received 16 July 2013; Accepted for publication 12 August 2013.

doi: 10.1111/jce.12270

Methods

Study Subjects

Between 1996 and 2012, a total of 1,373 probands were referred to our institutes (Shiga University of Medical Science and Kyoto University Graduate School of Medicine) for genetic testing. Among them, 7 cases had survived torsades de pointes (TdP) or ventricular fibrillation at ages < 1 year. This study enrolled these 7 infants. The QT interval was measured manually in leads II, V5, and V6, corrected by Bazett's formula,[16] and the longest value was used. A QTc interval >440 milliseconds was considered prolonged.[17] The protocols used for all investigations were in conformance with the principles outlined in the Declaration of Helsinki and were approved by the institutional ethics committee. The guardians